Physicochemical Conditions for Adsorption of Lead from Water by Rice Husk Ash

Chidozie Charles Nnaji,[a,*] Chinwe J. Ebeagwu,[a] and Emmanuel I. Ugwu [b]

The effects of physico-chemical parameters such as pH, temperature, and lead concentration on the efficiency of lead adsorption by rice husk ash were determined. Rice husk was incinerated at 800 °C for 6 h and then activated with 0.5 M HCl. Rice husk and rice husk ash (RHA) were characterized using scanning electron microscopy and X-ray fluorescence. Batch adsorption tests were conducted at different pH, temperature, and initial lead concentration. Kinetic studies were conducted at optimum pH of 3.0. The optimum lead removal of 80% was recorded at pH 3.0. Efficiency of lead removal by RHA decreased to 45% as pH increased to 9.0. Freundlich, Langmuir, Temkin, and Dubinin Radushkevich (D-R) isotherms performed acceptably well, with R^2 values of $0.954 \leq R^2 \leq 0.991$, $0.965 \leq R^2 \leq 0.996$, $0.949 \leq R^2 \leq 0.979$, and $0.970 \leq R^2 \leq 0.997$, respectively. Lead removal efficiency decreased from 75% to 50% as temperature increased from 30 °C to 40 °C. The adsorption of lead by RHA was by ion exchange in the acidic pH range and by physisorption in the alkaline pH range. Thermodynamic studies revealed that the process was exothermic and spontaneous and further confirmed the feasibility of the process with $-22.34 \leq \Delta G^0 \leq -24.94$. The intraparticle diffusion model and the pseudo first order kinetic model fit the experimental data very well, with average R^2 values of 0.985 and 0.987, respectively.

Keywords: Adsorption; Isotherm; Kinetics; Lead; Water; Rice husk ash; Temperature; pH

*Contact information: a: Department of Civil Engineering, University of Nigeria, Nsukka, Enugu State, Nigeria , b: Department of Civil Engineering, Michael Okpara University of Agriculture Umudike, P.M.B.7267 Umuahia Abia State, Nigeria; *Corresponding author: chidozie.nnaji@unn.edu.ng.*

INTRODUCTION

Heavy metals are regarded as priority pollutants due to their high mobility and persistence in the environment. Their presence has caused severe environmental problems due to their toxicity, even at low concentrations and insusceptibility to the environment. These heavy metals are not biodegradable and tend to accumulate in living organisms, causing various diseases and disorders. Lead is one of the three most toxic heavy metals that have dormant long-term negative impacts on health, causing hepatitis, anemia, nephritic syndrome, brain damage, mental deficiency, anorexia, vomiting, malaise, and encephalopathy (Deng *et al.* 2006). Lead affects human health and is a possible cause of human cancer (Lin *et al.* 1996). The significance of lead in environmental health has motivated numerous research works focusing on the use of cheap and available biosorbents to remove lead from aqueous solution (Lugo-Lugo *et al*. 2009; Naiya *et al.* 2009a; Singh and Das 2012; Singh *et al*. 2015).

Adsorption is an excellent way to treat contaminated water, offering advantages such as low-cost, greater availability, profitability, ease of operation, and effectiveness in reducing the concentration of heavy metal ions to very low levels (Demirbas 2008). Though activated carbon is the most popular and widely used adsorbent for heavy metal removal in water treatment applications, it is expensive, and its cost increases with quality (Babel and Kurniawan 2003). The need to reduce the cost of water treatment as well as minimize waste generation has led researchers

to explore the adsorption capacities of several waste materials. Pollutants can be absorbed from domestic and industrial wastewaters using materials of high internal surface area, with varying degrees of success depending on the nature of the pollutants and the adsorbent employed. The adsorption potentials of wood-based materials such as sawdust, wood stem, and wood bark have also been investigated (Seki *et al.* 1997; Tan and Xiao 2009). The sawdust of poplar wood, papaya wood, and *Pinus sylvestris* makes good heavy metal adsorbents (Saeed *et al.* 2005; Sciban *et al.* 2006; Sciban *et al.* 2007; Naiya *et al.* 2009c). Memon *et al.* (2007) used treated and untreated sawdust to achieve about 97% of Cd(II) removal within 8 min of contact. Agricultural wastes such as orange peels (Li *et al.* 2007), banana peels (Annadurai *et al.* 2003), mango peels (Iqbal *et al.* 2009), hazelnut shells (Cimino *et al.* 2000), peanut shells (Brown *et al.* 2000), rice husk, rice straw and rice bran (Ajmal *et al.* 2003; Singh and Das 2012), and neem leaf (Sharma and Bhattacharya 2005; Singh and Das 2012) have been employed successfully to remove heavy metals from wastewater. Crini (2006) outlined a number of other waste materials that have been effectively used as adsorbents and their relative performances in dye removal.

Rice husk, an agricultural waste material, is a major by-product of the rice milling industry and is one of the most commonly available lignocellulosic materials. The main components of rice husk are cellulose (25 to 35%), hemicelluloses (18 to 21%), lignin (26 to 31%), silica (15 to 17%), solubles (2 to 5%) and moisture (Luduena *et al.* 2011). Lignin, one of its major components, is a natural amorphous cross-linked resin that has an aromatic three-dimensional polymer structure containing phenolic, hydroxyl, carboxyl, benzyl alcohol, methoxyl, and aldehyde functional groups (Sarkanen and Ludwig 1971), making it potentially useful as an adsorbent material for the removal of heavy metals from water. Lignin consists of high quantity phenolic units and carboxyl groups that have higher affinity for heavy metal ions. This study undertook a comprehensive investigation of the physicochemical conditions for the adsorption of lead by rice husk ash (RHA), a low cost bio-sorbent made from rice husk which is an agricultural waste material. Equilibrium, thermodynamic and kinetic parameters were used to describe the sorption process.

EXPERIMENTAL

Collection of Sample and Activation of RHA

Rice husk was sourced from Adani rice milling station in Enugu State, Nigeria. The rice husk was sun dried for about two weeks and incinerated afterwards at a controlled temperature of about 800 °C for 6 h to obtain RHA. The ash was later sent to the National Geosciences Research Laboratory Kaduna, Nigeria, for chemical characterization. The RHA was washed with de-ionized water until no further impurities such as dust or residues were found and then dried in a vacuum oven at 103 °C. The RHA was activated chemically by soaking and slurry for 2 h using 0.5 M hydrochloric acid, followed by washing with de-ionized water and oven-drying for 3 h at 103 °C. The oven-dried RHA was milled in a porcelain jar to reduce the mean particle size and increase the specific surface area.

Batch Adsorption of Lead by RHA

The completely mixed batch reactor (CMBR) technique was used to investigate the adsorption of lead from water. Seven standard lead solutions with concentrations of 10, 30, 50, 70, 90, 110, and 130 mg/L were prepared. The pH was adjusted to 3.0 using a buffer solution and pH meter. Two hundred mg of adsorbent was added, stirred using mechanical shaker at room temperature for 3 h, and filtered using filter paper. The lead remaining in solution was quantified using a UV spectrophotometer (UV-1800 Shimadzu, Tokyo, Japan). All equipment and their

accessories as well as reagents used were made available by the National Centre for Energy Research and Development, University of Nigeria, Nsukka, Nigeria. The process was repeated at pH 5, 7, 8, and 9. The unused and spent adsorbents were subjected to Fourier Transform Infrared (FTIR) analysis. The removal efficiency (percentage of lead adsorbed) was estimated by Eq. 1,

$$\% \text{ Removal} = \frac{C_0 - C_e}{C_0} X100 \quad (1)$$

where C_0 and C_e are the initial and final concentrations of lead in the solution (mg/L), respectively. The optimum pH was noted. The adsorption experiment was repeated for the same range of lead concentrations and the optimum pH at 30 °C, 35 °C, and 40 °C. The amount of metal adsorbed per gram of the biomass was calculated as follows,

$$q_e = \frac{C_0 - C_e}{m} V \quad (2)$$

where q_e is the adsorption capacity at equilibrium (mg/g), m is the weight of adsorbent (g), V is the volume of metal solution (L), C_0 is the initial metal concentration(mg/L), and C_e is the metal concentration in solution at equilibrium (mg/L).

The experimental data were fitted to four isotherms namely: Langmuir, Freundlich, Temkin and Dubinin Radushkevich (D-R) isotherms. Adsorption isotherms provide insight into the sorption mechanisms, surface properties, and affinity of adsorbent (Khan *et al.* 2009). The Langmuir isotherm better describes monolayer adsorption, which assumes that the adsorbent surface is energetically homogeneous and that a monolayer surface coverage is formed with no interaction between the molecules adsorbed (Couto *et al.* 2015). The Freundlich isotherm recognizes the possibility of surface heterogeneity and intermolecular interactions between adsorbed molecules. Temkin isotherm assumes a linear decrease of heat of adsorption with coverage of adsorbent surface due to some indirect adsorbent/adsorbate interaction (Zheng *et al.* 2009). The D-R isotherm is generally applied to express the adsorption process occurred onto both homogenous and heterogeneous surfaces (Chen 2015). Both the linear and nonlinear forms of the four isotherms were used for fitting the results from the equilibrium studies (Table 1).

Table 1. Isotherm Models Fitted to Experimental Data

Isotherm	Linear Form	Nonlinear Form
Langmuir	$\frac{C_e}{q_e} = \frac{1}{q_m K_L} + \frac{C_e}{q_m}$	$q_e = q_m K_L \frac{C_e}{1 + K_L C_e}$
Freundlich	$\ln q_e = \ln K_F + \frac{1}{n} C_e$	$q_m = K_F C_e^{1/n}$
Temkin	$q_e = B \ln A + B \ln C_e$ *Where* $B = \frac{RT}{b}$	$q_e = B \ln(AC_e)$
D-R	$\ln q_e = \ln q_s - \beta\varepsilon^2$ *Where* $\varepsilon = RT \ln\left(1 + \frac{1}{C_e}\right)$	$q_e = q_s \exp(-\beta\varepsilon^2)$

In Table 1, C_e (mg/L) is the amount of solute in solution at equilibrium, q_e (mg/L) is the amount of solute adsorbed per unit mass of adsorbent at equilibrium, q_m (mg/g) is the monolayer adsorption capacity, and K_L(L/mg) is the equilibrium adsorption constant, which is a measure of

adsorption affinity. K_F is the Freundlich constant, which is indicative of the relative adsorption capacity of the adsorbent (mg/g), while n is the heterogeneous factor related to the adsorption intensity of the adsorbent. The constant b (J/mmol) in the Temkin isotherm is related to the heat of adsorption, A (L/mmol) is the Temkin isotherm constant, R is the universal gas constant with a value of 8.314J/mol/K and T is absolute temperature, q_s(mol/g) is the theoretical monolayer sorption capacity and β(mol^2/J^2) is the constant which is related to the mean sorption energy (E). The mean sorption energy E (kJ/mol) gives information regarding the nature of the adsorption process. The value of E is estimated using the expression given in Eq. 3.

$$E = \frac{1}{\sqrt{2\beta}} \tag{3}$$

Thermodynamic parameters were computed using the thermodynamic law given in Eq. 4,

$$\Delta G^0 = -RT \ln K_a \tag{4}$$

where ΔG^0(J/mmol) is Gibb's energy change which is normally used to determine the feasibility and spontaneity of the adsorption process and is given as Eq. 5, R is the universal gas constant (8.314J/mol/k), T is absolute temperature (K), and K_a is the thermodynamic equilibrium constant.

$$\Delta G^0 = \Delta H^0 - T\Delta S^0 \tag{5}$$

Substituting Eq. 4 into Eq. 5 yields Eq. 6,

$$\ln K_a = \frac{\Delta S^0}{R} - \frac{\Delta H^0}{RT} \tag{6}$$

where ΔH^0 (J/mol) represents enthalpy change, which indicates whether the process is exothermic ($\Delta H^0 < 0$) or endothermic ($\Delta H^0 > 0$) and ΔS^0(J/mmol/K) is the change in entropy. The thermodynamic equilibrium constant was taken as the Langmuir equilibrium constant, K_L as recommended by Liu (2009).

Kinetic Studies

For the kinetic studies, seven standard lead solutions with concentrations of 10, 30, 50, 70, 90, 110, and 130 mg/L were prepared, and the pH was adjusted to the optimum pH of 3.0. The amount of lead adsorbed at various time intervals was recorded. Five sorption kinetic models were used to model the rate of sorption of lead by RHA, including the first order kinetic, second order kinetic, pseudo first order kinetic, pseudo second order kinetic, and the inter particle diffusion models. The first order kinetic model assumes that the rate of sorption is proportional to solute concentration while the second order kinetic model assumes that the rate of sorption is proportional to the square of solute concentration. The first order kinetic model and its integrated form are given respectively in Eq. 7 and Eq. 8.

$$\frac{dC}{dt} = -KC \tag{7}$$

$$Ln\frac{C_0}{C} = Kt \tag{8}$$

The second order kinetic model and its integrated form are given respectively in Eq. 9 and Eq. 10,

$$\frac{dC}{dt} = -KC^2 \quad (9)$$

$$\frac{1}{C} = \frac{1}{C_0} + Kt \quad (10)$$

where C is the solute concentration in solution (mg/L) at time t (min) and K is the rate constant. The pseudo first order kinetic model assumes that the rate of sorption is proportional to the deficit in equilibrium concentration of solute in the adsorbent, as follows,

$$\frac{dq_t}{dt} = K(q_e - q_t) \quad (11)$$

where q_t represents the amount of solute adsorbed per gram of the adsorbent (mg/g) and q_e is the equilibrium concentration of solute in the adsorbent (mg/g). The term (q_e – q_t) represents the sorption driving force. In the same vein, the integrated and linearized form of the pseudo second order kinetic model is given in Eq. 12.

$$\frac{t}{q_t} = \frac{1}{Kq_e^2} + \frac{t}{q_e} \quad (12)$$

The inter particle diffusion model is given as Eq. 13,

$$q_t = K_p\sqrt{t} + I_d \quad (13)$$

where K_p is the initial rate of inter particle diffusion and I_d is the model constant.

RESULTS AND DISCUSSION

Characterization of Incinerated Rice Husk

When rice husk is burnt at 550 °C to 800 °C, a highly porous mass consisting mostly of amorphous silica is formed. Rice husk is brownish in colour, but after burning at 800 °C, it produced a grayish to whitish residue. The silica content of RHA used in this study was 72%. A scanning electron micrograph of RHA is shown in Fig. 1, while the chemical composition is shown in Tables 2 and 3. The internal structure of RHA contained a number of irregular pieces of honeycombed multi-layered and angular orientation. The porous structure of RHA had a relatively large specific surface area, and this morphological property is conducive to the uptake of metal ions (Zhang *et al*. 2014).

Table 2. Chemical Composition of Rice Husk and RHA

Compound	SiO_2	AL_2O_2	P_2O_5	SO_3	Na_2O	K_2O	CaO	MgO	TiO_2	Fe_2O_3	LOI
RH (%)	41.6	<0.001	11.2	1.5	2.01	5.23	3.8	0.06	0.82	3.12	29.04
RHA (%)	72.2	<0.001	9.46	<0.001	0.84	1.7	2.94	0.8	0.645	2.4	N/A

Table 3. Rare Earth Metals in Rice Husk

Metal	RH	RHA	Metal	RH	RHA
V	0.001	0.01	Yb	<0.001	0.02
Cr	<0.001	0.001	Zr	<0.001	<0.001
Cu	0.01	0.05	Eu	<0.001	0.09
Zn	0.10	0.33	Hg	<0.001	0.03
Ni	0.001	0.033	Rb	0.001	0.078
Sr	<0.001	<0.001	Pb	<0.0	<0.0

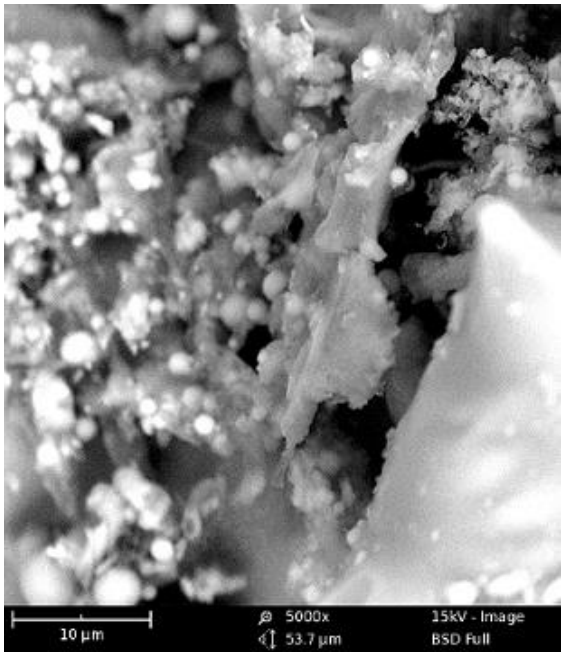

Fig. 1. SEM of RHA

Efficiency of Lead Adsorption by RHA

FTIR analyses confirmed the presence of functional groups, which played major role in the adsorption process (Table 4). After adsorption some of the observed peaks shifted, while some disappeared entirely, thereby confirming the occurrence of metal binding on the surface of the adsorbent. The shifts from 3585.42 cm^{-1} and 3107.4 cm^{-1} for unused RHA to 3415.8 cm^{-1} and 3169.08 cm^{-1} respectively for spent RHA suggest the participation of the O-H functional groups in the process. There was also a shift from 1133.64 cm^{-1} to 1125.93 cm^{-1} after adsorption, which can be attributed to the C-O functional groups, while the shift from 1462.62 cm^{-1} to 1395.78 can be attributed to the C-H bending of alkenes. Chaouch *et al.* (2014) noted that the removal of metal ions from an aqueous solution by adsorption is highly dependent on the solution pH. This also affects the surface charge on the adsorbent and the degree of ionization and speciation of the adsorbent. The solution pH determines both the predominant species and the net charge on the surface of the adsorbent (Couto *et al.* 2015). Higher adsorption efficiencies were recorded at low pH. The highest recorded lead removal efficiency was 80% at pH 3.0, which is equivalent to a sorption capacity of 0.061 mmol/g (12.75 mg/g). The efficiency of adsorption decreased to 45% at a pH of 9.0. Figure 2 suggests that a unit drop in pH led to a 5% increase in adsorption efficiency. Figure 2 also shows that the adsorption of lead by RHA was highly pH-dependent for dilute solutions. In fact, adsorption process is generally pH and solute specific. Mashhadi *et al.* (2016)

reported that the sorption of methylene blue by activated carbon made from rice straw attained optimum performance at pH 7.0, while Agarwal *et al*. (2016) reported optimum pH values of 6.0, 8.0 and 9.0 for the sorption of methylene blue by *E. strobilacea* char, *Ephedra strobilacea* char, and *E. strobilacea* char respectively. However, for a concentrated solution of 130 mg/L, the adsorption process appeared to be independent of pH. Generally, higher removal efficiencies were observed at lower adsorbate concentrations, but higher adsorption capacities were observed at higher adsorbate concentration. Singh *et al.* (2009) also found that arsenic (III) adsorption was favoured at low solute concentration. Under certain conditions, there is an increase in removal efficiency with increased pH (Chaouch *et al.* 2014; Zeng *et al.* 2015); at high pH, the adsorbent surface assumes a net negative charge, which favours the attraction and subsequent adsorption of positively charged ions.

Cozmuta *et al.* (2012) observed that lead complexes favoured at low pH have smaller hydrated radii and are therefore more mobile than the normal lead ion. Moreover, as pH increases, competition for adsorption sites ensues between the hydrogen ion and the lead ion, thus reducing adsorption efficiency. This implies that pH has more effect on adsorption in dilute metal solutions than in concentrated ones, as demonstrated by Fig. 2. Hence, two practical approaches for the application of RHA to lead adsorption can be proposed. One approach is to dilute the solution to about 10 mg/L for optimum removal efficiency. Alternatively, for better performance and optimum utilization of the adsorbent, a concentrated solution can be subjected to batches of adsorbent in sequence.

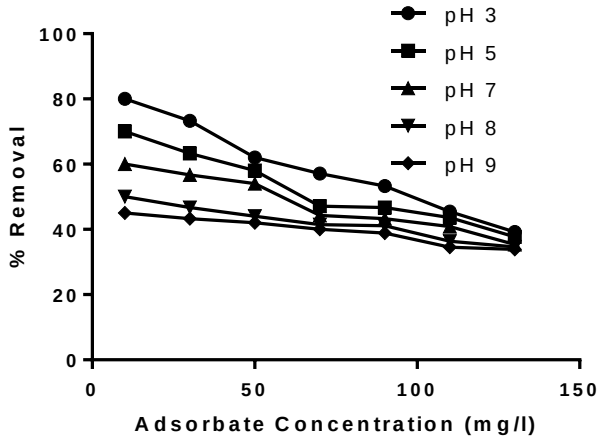

Fig. 2. Plots of lead adsorption by RHA at different pH

Table 4. Identification of Main Functional Groups by FTIR

Band Position (cm^{-1})		Possible Assignment
Activated RHA	Spent Activated RHA	
486	455.16	S-S stretching of disulfides
578.52	-	C-S stretching of disulfides
1133.64	1125.93	C-O stretching of alcohols
1462.62	1395.78	C-H bending of alkenes
1627.08	1627.08	C=C stretching of alkenes
2028	-	-NCS isothiocyanate
2999.46	-	C-H stretching
3107.4	3169.08	OH stretching of carboxylic acids
3277.02	-	O-H stretching of alcohols
3585.42	3415.8	O-H stretching of phenols
3785.88	-	

Isotherm of Lead Removal by RHA

Figures 3 and 4 show that all four isotherms described the adsorption mechanism very well with $0.954 \leq R^2 \leq 0.991$, $0.965 \leq R^2 \leq 0.996$, $0.949 \leq R^2 \leq 0.979$ and $0.970 \leq R^2 \leq 0.997$ for Freundlich, Langmuir, Temkin, and D-R isotherms respectively (Table 5). The parameters of both Freundlich and Langmuir isotherms are plotted in Fig. 5. The parameters of the Freundlich isotherm (n and K) generally decreased as pH increased. For the Langmuir isotherm, the monolayer adsorption capacity (q_m) increased as pH increased. However, this increase in monolayer adsorption capacity was neutralized by the reduction in adsorption affinity as pH increased. Hence, though the adsorbent had the capacity to accommodate more solute at high pH, the mechanisms that initiate the adsorption of lead onto RHA were not favoured at high pH.

Table 5. Summary of Isotherm Parameters for Different pH using Linear and Nonlinear Fitting

Isotherm	Parameter	pH									
		Nonlinear Fitting					Linear Fitting				
		3	5	7	8	9	3	5	7	8	9
Freundlich	K	2.38	1.44	1.09	0.57	0.47	1.63	1.03	0.68	0.38	0.29
	n	2.48	2.00	1.83	1.48	1.40	1.96	1.69	1.49	1.28	1.20
	R^2	0.954	0.973	0.971	0.986	0.988	0.964	0.976	0.971	0.991	0.991
Langmuir	q_m (mmol/g)	0.076	0.081	0.083	0.108	0.115	0.074	0.079	0.084	0.111	0.126
	K_L (L/mmol)	12.72	6.90	5.18	2.46	2.02	13.98	7.48	5.04	2.37	1.75
	R^2	0.987	0.981	0.986	0.995	0.996	0.993	0.976	0.977	0.980	0.965
Temkin	B	3.12	3.31	3.43	3.60	3.61	3.12	3.31	3.43	3.60	3.61
	A (L/mmol)	171.71	96.04	67.07	44.53	39.18	171.70	96.03	67.06	44.53	39.17
	R^2	0.979	0.965	0.970	0.949	0.949	0.979	0.965	0.970	0.949	0.949
D-R	β ($\times 10^{-8}$ mol^2/Jol^2)	0.363	0.457	0.507	0.642	0.678	0.496	0.587	0.679	0.798	0.852
	q_s (mmol/g)	0.263	0.348	0.391	0.610	0.669	0.364	0.445	0.567	0.765	0.876
	E (kJ/mol)	11.744	10.461	9.930	8.827	8.585	10.039	9.229	8.584	7.917	7.661
	R^2	0.970	0.979	0.979	0.991	0.993	0.981	0.987	0.984	0.997	0.997

The maximum monolayer adsorption capacities ranging from 0.074 mmol/g (15.33 mg/g) to 0.126 mmol/g (26.11 mg/g) were lower than those obtained for the adsorption of lead by the sepiolite (30.5 mg/g) as reported by Sharifipour *et al.* (2015) but they were much higher than that (0.612 mg/g) obtained for the adsorption of lead from wastewater using RHA. Table 6 shows that activated RHA had higher lead adsorption capacity than apricot stone and hazelnut husk but lower adsorption capacity than cotton stalk and coconut shell. The values of the Freundlich number (n) obtained in this study (Tables 5 and 7) are all greater than 1.0 which is indicative of the favorability of the process. Value of $n = 1$ suggests that the partition of solute between solid and liquid phases are independent, values of $n > 1$ indicate normal adsorption, while $n < 1$ indicates cooperative adsorption (Mohan and Karthikeyan 1997). The value of n was highest at pH 3.0 with a value of 2.48 and lowest at pH 9.0 with a value of 1.40 (Table 5). This confirms that the adsorption of lead by RHA was more favourable at low pH. Generally, Langmuir isotherm performed better than all other isotherms in all cases for nonlinear fitting, while D-R isotherm performed better than the other isotherms in all cases except at pH 3.0 for linear fitting. The linear Langmuir isotherm

performed better than the others at pH. 3.0. Numerous studies have reported the suitability of the Langmuir isotherm for describing adsorption of heavy metals to natural and synthetic adsorbents. Naiya *et al.* (2009b) found that the sorption of Cd (II) and Pb (II) by modified orange peel was best described by Langmuir isotherm. Ghasemi *et al.* (2016a) also reported that the adsorption of Ni by zeolite followed Langmiur isotherm. On the contrary, Naiya *et al.* (2009a) found that Freundlich isotherm was more appropriate for the sorption of Pb(II) by clarified sludge.

Table 6. Comparison of Lead Adsorption Capacity of RHA with Other Bio-sorbents

Adsorbent	Adsorption Capacity (mg/g)	Reference
Soybean hulls	39.37	Johns *et al.* (1998)
Pecan Shell	64.2	Bansode et al (2003
Coconut shell	76.6	Kikuchi *et al.* (2006)
	26.5	Sekar *et al*. (2004)
Apricot stone	22.85	Kobya *et al.* (2005)
	21.38	Mouni *et al.* (2011)
Hazelnut husk	13.03	Imamoglu and Tekir (2008)
Palm nut shell	95.2	Issabayeva *et al*. (2006)
Soybean oil cake	476.2	Erdem *et al*. (2013)
Cotton stalk	119	Li *et al.* (2010)
Peanut shell	35.5	Xu and Liu (2008)
Rice husk ash	26.11	This study

Table 5 shows that the linear isotherms generally performed better than their nonlinear counterpart except for the Temkin and Langmuir isotherms. While nonlinear Langmuir isotherm performed better than its nonlinear counterpart at all pH except pH 3.0, the linear and nonlinear Temkin isotherms yielded identical results, as can be clearly observed in Table 5.

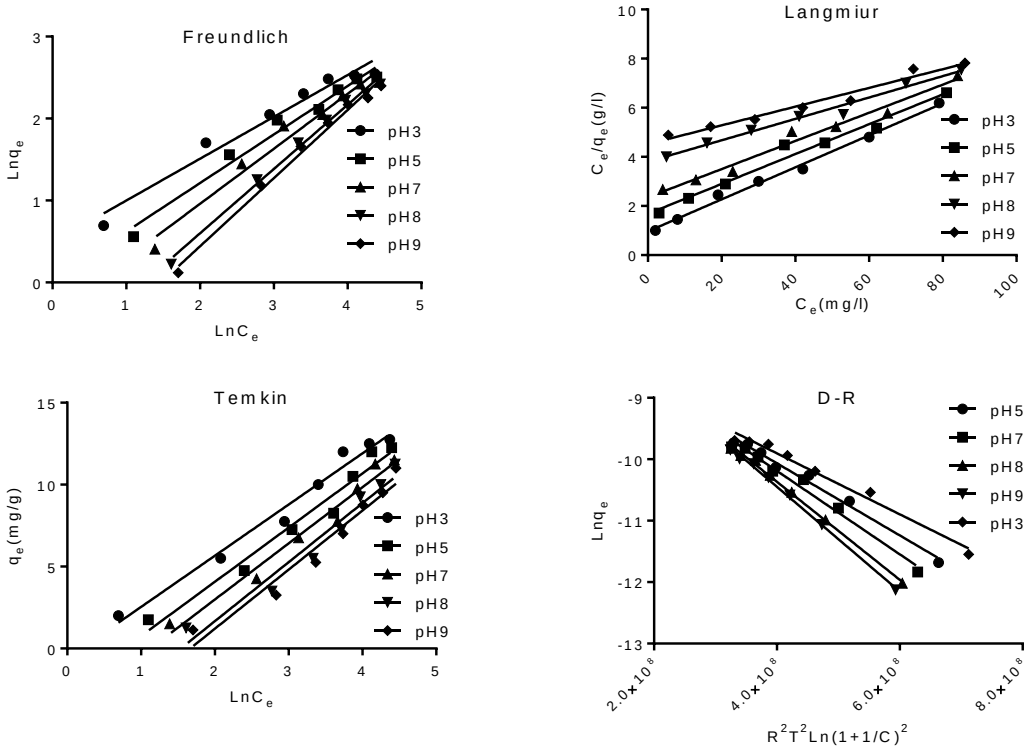

Fig. 3. Linear fitting of adsorption isotherms at different pH

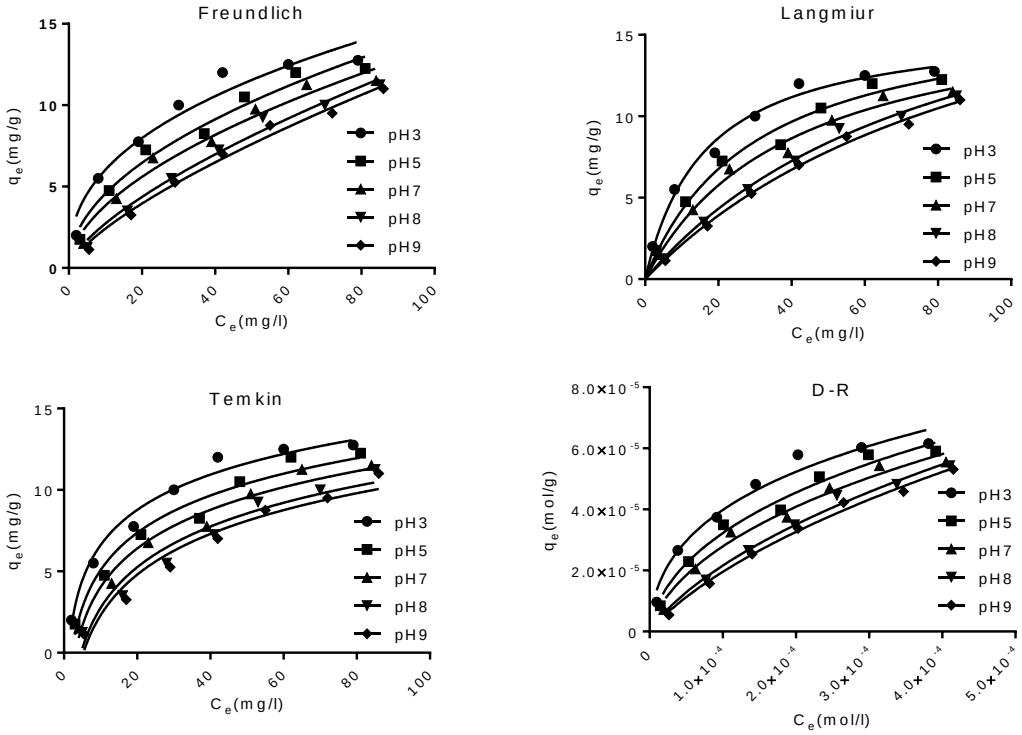

Fig. 4. Non-linear fitting of adsorption isotherms at different pH

The effect of temperature on adsorption was studied at 30 °C, 35 °C, and 40 °C at pH 3.0. For an initial lead concentration of 10 mg/L, the removal efficiencies were 75%, 60%, and 50% at 30 °C, 35 °C, and 40 °C, respectively. The decrease in lead adsorption efficiency by RHA as temperature increased suggests that the process is exothermic and is therefore favoured at lower adsorption temperatures. Table 7 in conjunction with Figs. 6 and 7 shows that lead adsorption onto RHA followed a Langmuir isotherm for both linear and nonlinear fitting and all ranges of temperatures studied except for temperature of 40 °C in which the linear D-R isotherm performed better than others. Table 7 also shows that the Freundlich constant (*n*) decreased from 2.31 at 30 °C to 1.68 at 40 °C for nonlinear fitting and from 1.79 to 1.33 for linear fitting. Hence the value of *n* was inversely proportional to temperature which implies that the process became less favourable as temperature increased. The favourability of the process was further investigated using the dimensionless parameter R_L estimated by Eq. 14, where $R_L = 0$ suggests that the adsorption process is irreversible; $0 < R_L < 1$ denotes a favourable process; $R_L = 1$ suggests that the process is linear; and $R_L > 1$ suggests that the adsorption process is unfavourable (Zeng *et al.* 2015).

$$R_L = \frac{1}{1 + bC_0} \tag{14}$$

The dimensionless parameter R_L increased from 0.66 at 30 °C to 0.87 at 40 °C. Over the three ranges of temperature studies, R_L increased by approximately 0.105 for every 5 °C increase in temperature. Following this trend, the value of R_L will exceed 1.0 at about 47 °C, at which point the adsorption process becomes unfavourable.

Table 7. Summary of Isotherm Parameters at Different Temperatures

Isotherm	Parameters	Temp(K) 30°C	35°C	40°C	30°C	35°C	40°C
		Non Linear			Linear		
Freundlich	*K*	2.01	1.46	0.77	1.285	0.731	0.430
	n	2.31	2.07	1.68	1.79	1.49	1.33
	R^2	0.941	0.929	0.968	0.964	0.944	0.965
Langmuir	q_m (mmol/g)	0.077	0.077	0.083	0.075	0.080	0.091
	K_L (L/mmol)	10.07	7.25	3.91	10.80	6.31	3.20
	R^2	0.983	0.983	0.982	0.9881	0.9682	0.939
Temkin	*B*	3.27	3.49	3.37	3.27	3.49	3.37
	A (L/mmol)	125.50	73.25	49.89	125.50	73.25	49.89
	R^2	0.968	0.979	0.968	0.968	0.979	0.968
D-R	β(x10^{-8} mol^2/Jol^2)	0.40	0.45	0.56	0.55	0.68	0.77
	q_s (mmol/g)	0.288	0.321	0.423	0.420	0.609	0.680
	E (kJ/mol)	11.248	10.550	9.454	9.547	8.574	8.070
	R^2	0.957	0.948	0.975	0.9797	0.9641	0.978

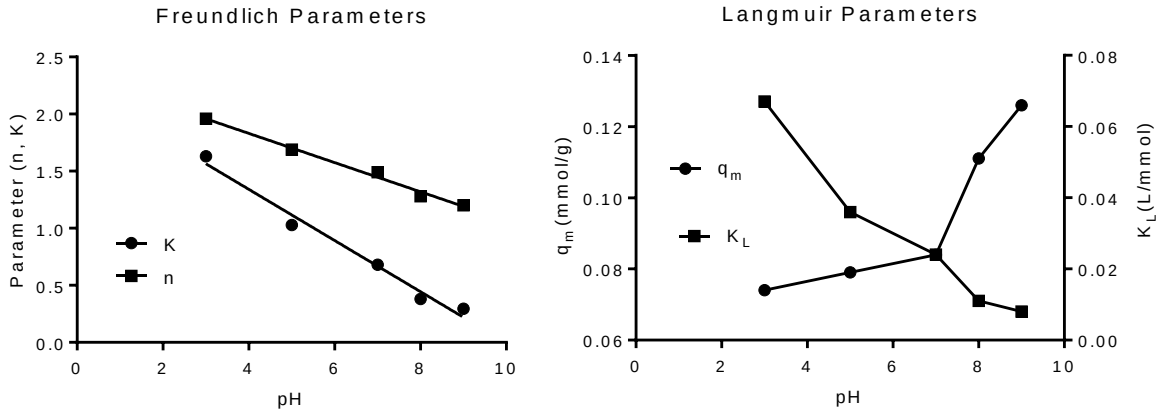

Fig. 5. Parameters of (a) Freundlich isotherm and (b) Langmuir isotherm

The nature of the sorption process was investigated using the mean sorption energy (*E*) estimated with Eq. 3. The mean sorption energy ranged from 8.85 kJ/mol at pH 9.0 to 11.74 kJ/mol at pH 3.0 for nonlinear fitting and from 7.66 kJ/mol at pH 9.0 to 10.04 kJ/mol at pH 3.0 for linear fitting. Similarly, the mean sorption energy ranged from 9.45 kJ/mol at 40 °C to 11.25 kJ/mol at 30 °C for nonlinear fitting and from 7.66 kJ/mol at 40 °C to 10.04 kJ/mol at 30 °C for linear fitting. These values are similar to those obtained by Naiya *et al*. (2009a) for the sorption of lead by clarified sludge (11.8 kJ/mol) and Lugo-Lugo (2009) for the sorption of lead by orange peel (10.17 kJ/mol). Values of $E < 8$ kJ/mol indicate physical adsorption, 8 kJ/mol < E < 16 kJ/mol signify an ion exchange process, E < 20 kJ/mol < 40 kJ/mol signify chemisorption (Ghasemi *et al.* 2016b).The values of *E* obtained in this study suggest that the sorption of lead by RHA is an ion

exchange process at low pH but becomes a physical process at high pH (Table 5). Table 7 shows that sorption process approaches physisorption as temperature increases. Going by the linear fitting of the D-R isotherm, the adsorption process was by ion exchange in the acidic pH range and physical sorption in the alkaline pH range.

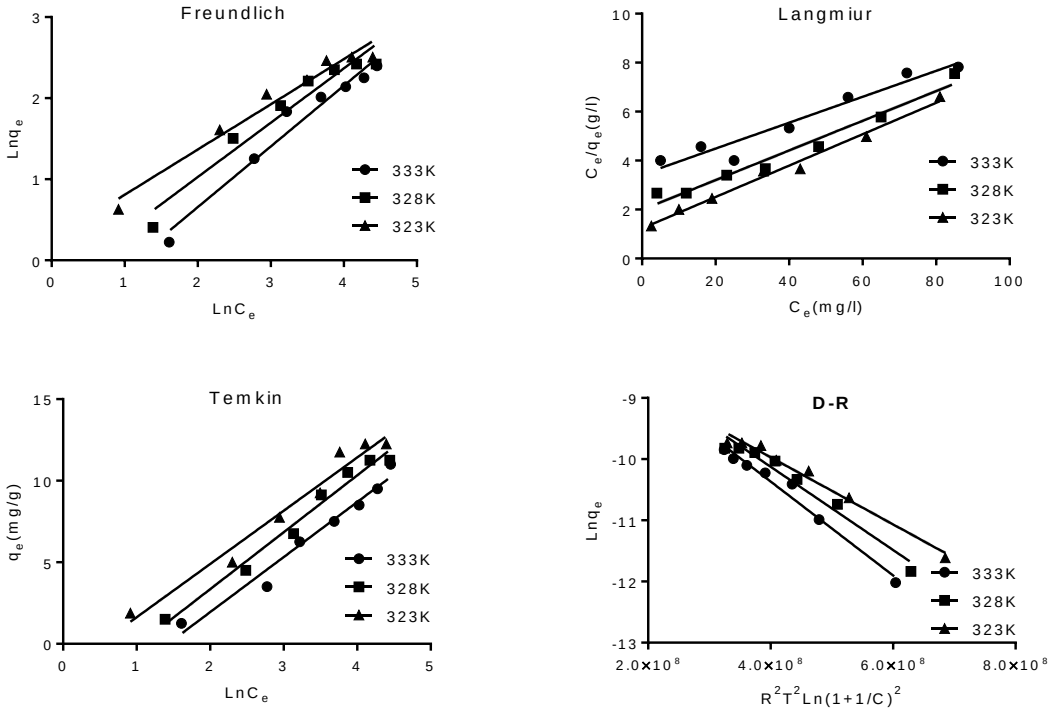

Fig. 6. Linear fitting of adsorption isotherms at different temperatures

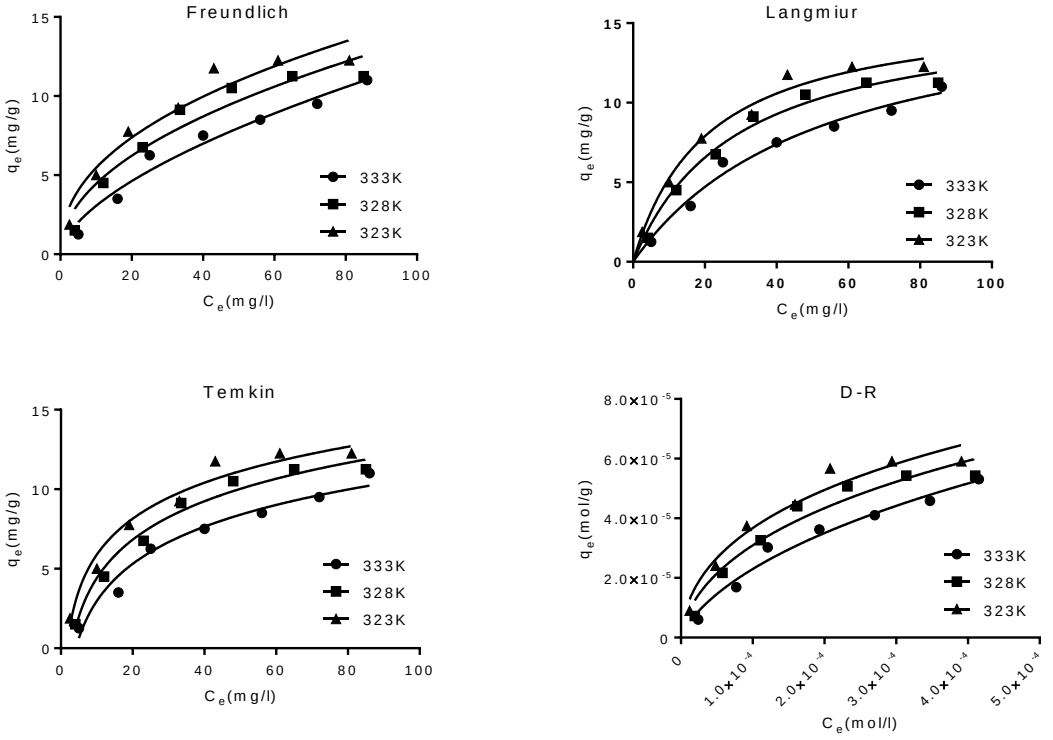

Fig. 7. Non-linear fitting of adsorption isotherms at different temperatures

Thermodynamics of Lead Adsorption by RHA

The values of ΔG^0 at various temperatures were calculated using Eq. 4, while the values of ΔH^0 and ΔS^0 were, respectively, obtained from the slope and intercept of the plot of $\ln K_L$ versus $1/T$ (Fig. 8). Values of ΔG^0 obtained for the various temperatures considered ranged between -22.34 and -24.94kJ/mol. The negative values of ΔG^0 indicate that the adsorption of lead to RHA is both feasible and spontaneous, thereby confirming the favourability of the process. It should be noted that the process is more energetically favoured at lower temperature as portrayed by the increasing negative values of ΔG^0 as temperature decreases (Table 8). The negative values of ΔH^0 obtained reveal that the process is exothermic. Tran and Chao (2016) observed that exothermic adsorption processes that release heat to the surrounding involve either physisorption or chemisorption or both, while endothermic adsorption processes unequivocally indicate chemisorption. Several adsorption studies reported the same range of thermodynamic values (Liu 2009; Tran and Chao 2016; Ghasemi *et al*. 2016a). The negative values of ΔS^0 suggest that the sorption process is enthalpy driven and that an increased disorder at the solid/liquid interface caused the adsorbate ion/molecules to escape from the solid phase to the liquid phase (Ghasemi *et al*. 2016a).

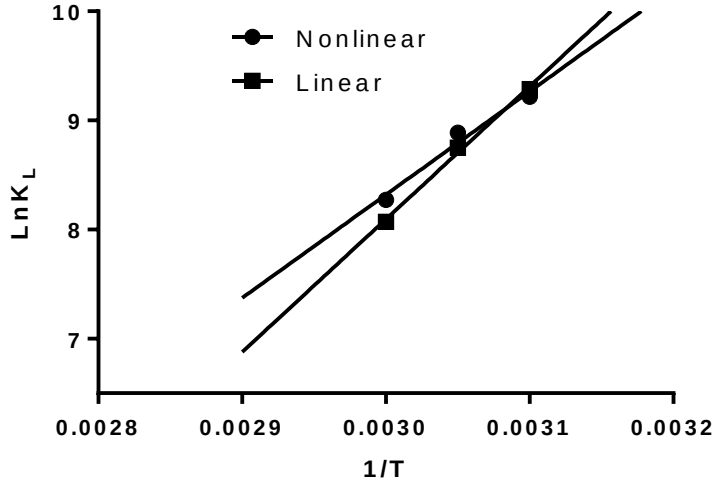

Fig. 8. Plot of $\ln K_L$ against $1/T$

Table 8. Thermodynamic Parameters Calculated with K_L from Linear and Non-linear Fitting of Langmuir iIsotherm

T (K)	Δ*G* (kJ/mol)	R^2	Δ*S* (J/mol/K)	Δ*H* (kJ/mol)	Δ*G* (kJ/mol)	R^2	Δ*S* (J/mol/K)	Δ*H* (kJ/mol)
	Non-Linear Fitting				Linear Fitting			
30°C	-24.75				-24.94			
35°C	-24.24	0.967	-184.45	-84.46	-23.86	0.994	-259.95	-108.8
40°C	-22.90				-22.34			

Kinetics of Lead Removal by RHA

All five models fitted the data adequately with R^2 values ranging between 0.91 and 0.995 (Fig. 9). A summary of the performance of the models for different lead concentrations are given in Table 9. The pseudo second order and first order kinetic models were found to best describe the rate of sorption for dilute lead solution (C_0 = 10 mg/L) with R^2 = 0.978).

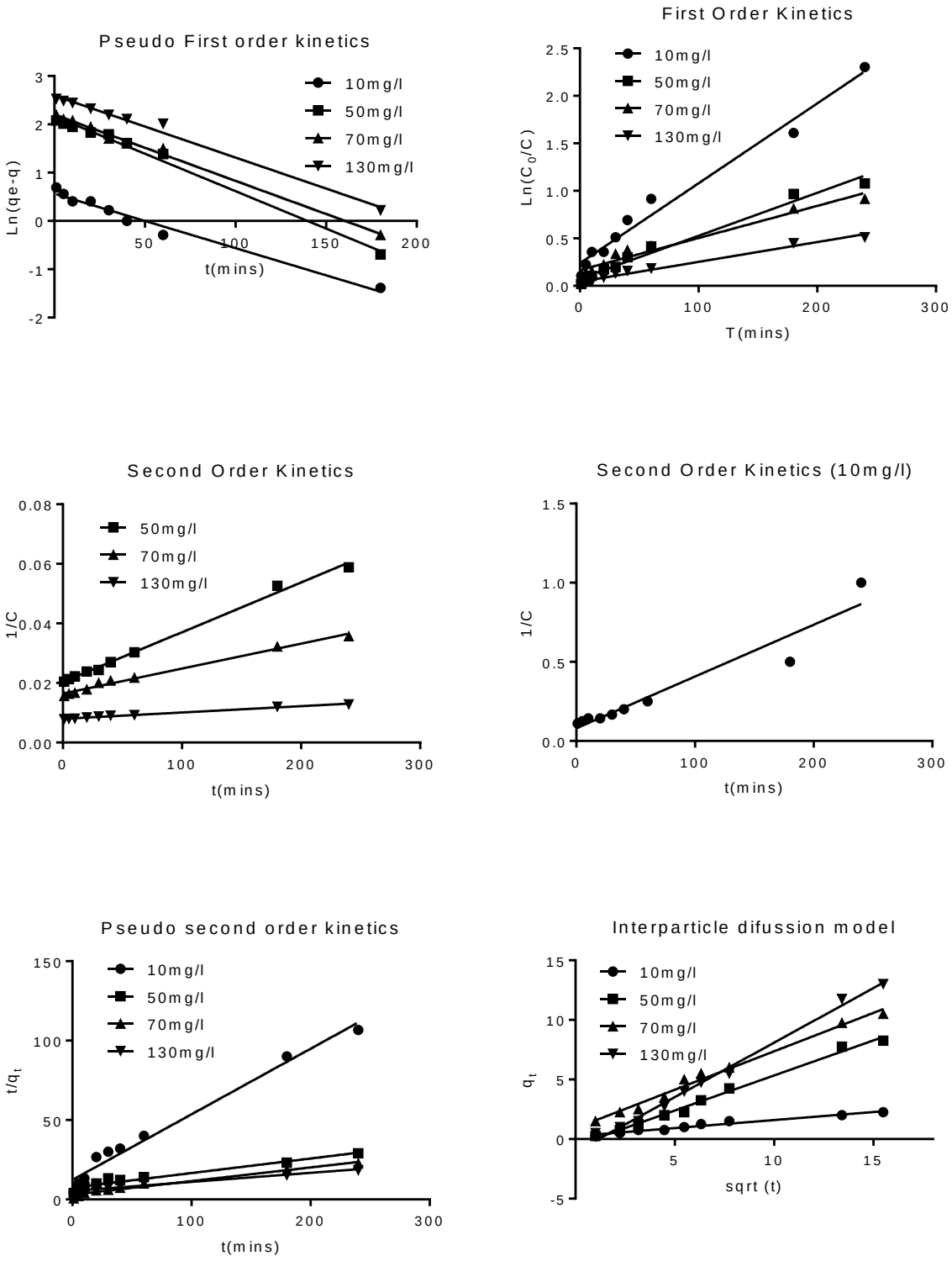

Fig. 9. Plots of kinetic models for lead adsorption by RHA

The second order and the pseudo first order kinetic models were more suitable for intermediate lead concentrations of 50 mg/L and 70 mg/L, respectively. The interparticle diffusion model best described sorption at higher lead concentration (C_0 = 130 mg/L), with an R^2 of 0.99. The first order, second order and pseudo second order sorption rate constants decreased as initial lead concentration increased while the intraparticle sorption rate constant increased with concentration. However, the pseudo first order sorption rate constant increased from 0.0113 min^{-1} at an initial lead concentration of 10 mg/L to a maximum value of 0.155min^{-1} at 50 mg/L and then decreased to 0.0128 min^{-1} at 130 mg/L. The values of the kinetic rate constants fall within the range reported by other researchers. Sharifipour *et al.* (2015) reported that the pseudo first order sorption rate constant for the sorption of lead was 0.0046 min^{-1} and 0.0023 to 0.0046 m^{-1} for sepiolite and zeolite respectively, while the pseudo second order sorption rate constant was 0.0032 to 0.005g/mg/min and 0.0045 to 0.0066 g/mg/min for sepiolite and zeolite respectively. These values are clearly far below the pseudo first order rate constants but fall within the pseudo first order rate constants obtained in this study. However, Hikmat *et al.* (2014) obtained first order sorption rate constants which are far above those obtained in this study.

The overall performance of the kinetic models is presented in Fig. 10, showing that the pseudo first order kinetic and the inter particle diffusion models performed better than the other kinetic models. The discrepancies in the performance of the models can be attributed to their structural differences. While the first order and second order kinetic models focus on what is happening in the liquid phase, the pseudo first order, pseudo second order, and inter particle diffusion kinetic models focus on what is happening in the solid phase within the adsorbent. Hence, at a low concentration where solute might be a limiting factor, the first order and second order kinetic models perform better. However, at high solute concentration, the sorption process is controlled by the availability of sorption sites in the adsorbent, thus favouring pseudo first order, pseudo second order and inter particle diffusion kinetic models.

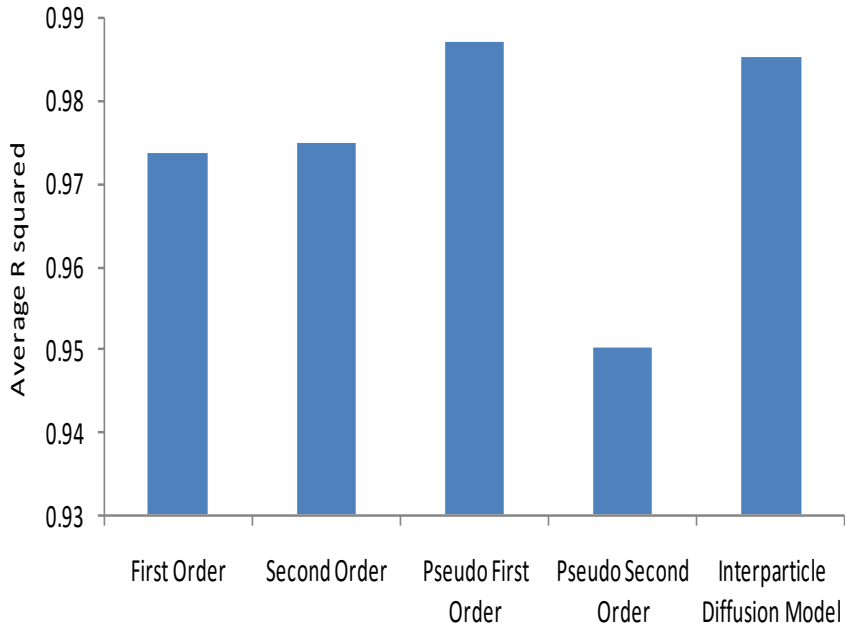

Fig. 10. Comparison of average performance of kinetic models

Table 9. Sorption Rate Constants of Various Kinetic Models for Different Lead Concentration

Initial Concentration (mg/l)	First order		Pseudo first order		Second order		Pseudo second order		Intraparticle diffusion	
	k (min^{-1})	R^2	k (min^{-1})	R^2	k (l/mg min)	R^2	k (g/mg min)	R^2	k (g/mg min^{-1})	R^2
10	0.0084	0.978	0.0113	0.975	0.0033	0.926	0.0138	0.978	0.135	0.969
50	0.0045	0.980	0.0155	0.991	0.00017	0.995	0.0011	0.946	0.588	0.992
70	0.0034	0.958	0.0137	0.994	0.000084	0.988	0.0025	0.970	0.645	0.987
130	0.0021	0.978	0.0128	0.988	0.000021	0.991	0.00061	0.909	0.915	0.993

CONCLUSIONS

1. The threat posed by lead in industrial wastewater can be curtailed by using acid-treated rice husk ash (RHA) as a cheap and abundantly available adsorbent.
2. By controlling physicochemical parameters such as pH, temperature, and initial lead concentration, a high lead removal efficiency by RHA can be achieved.
3. Low pH and moderate temperatures favour the adsorption of lead onto RHA.
4. The effect of pH on the adsorption process was more pronounced in dilute solutions.
5. The sorption of lead by RHA is a feasible and spontaneous exothermic process
6. Langmuir, Freundlich, Temkin, and D-R isotherms fit the experimental data very well.
7. The sorption process occurs by ion exchange in the acidic pH range and by physisorption in the alkaline pH range.
8. The pseudo first order kinetic and the inter particle diffusion models described the rate of sorption acceptably.

REFERENCES CITED

Agarwal, S., Tyagi, I., Gupta, V. K., Ghasemi, N., Shahiavand, M., and Ghasemi, M. (2016) "Kinetics, equilibrium studies and thermodynamics of methylene blue adsorption on *Ephedra strobilacea* saw dust and modified using phosphoric acid and zinc chloride," *Journal of Molecular Liquids* 218, 208-218.

Ajmal, M., Rao, R. A. K., Anwar, S., Ahmad, J., and Ahmad, R. (2003). "Adsorption studies on rice husk: Removal and recovery of Cd(II) from wastewater," *Bioresource Technology* 86(2), 147-149. DOI: 10.1016/S0960-8524(02)00159-1

Annadurai, G., Juang, R. S., and Lee, D. L. (2003). "Adsorption of heavy metals from water using banana and orange peels," *Water Science Technology* 47(1), 185-190.

Babel, S., and Kurniawan, T. A., (2003). "Low-cost adsorbents for heavy metals uptake from contaminated water: A review," *Journal of Hazardous Materials* 97(1-3), 219-243. DOI: 10.1016/S0304-3894(02)00263-7

Bansode, R. R., Losso, J. N., Marshall, W. E., Rao, R. M., and. Portier, R. J. (2003). "Adsorption of metal ions by pecan shell-based granular activated carbons," *Bioresource Technology* 89(2), 115-119.

Brown, P., Jefcoat, I. A., Parrish, D., Gill, S., and Graham, E. (2000). "Evaluation of the adsorptive capacity of peanut hull pellets for heavy metals in solution," *Advances in Environmental Research* 4(1), 19-29. DOI: 10.1016/S1093-0191(00)00004-6

Chaouch, N., Ouahrani, M. R., and Laouini, S. E. (2014). "Adsorption of lead (II) from aqueous solutions onto activated carbon prepared from Algerian dates stones of *Phoenix dactylifera* L. (Ghars variety) by H_3PO_4 activation," *Oriental Journal of Chemistry* 30(3), 1317-1322. DOI: 10.13005/ojc/300349

Chen, X. (2015). "Modeling of experimental adsorption isotherm data," *Information* 6, 14-22.

Cimino, G., Passerini, A., and Toscano, G. (2000). "Removal of toxic cations and Cr(VI) from aqueous solution by hazelnut shell," *Water Research* 34(11), 295-2962. DOI: 10.1016/S0043-1354(00)00048-8

Couto, O. M., Matos, I., da Fonseca, I. M., Arroyo, P. A., da Silva, E. A., and de Barros, M. A. (2015). "Effect of solution pH and influence of water hardness on caffeine adsorption onto activated carbons," *The Canadian Journal of Chemical Engineering* 93(1), 63-77. DOI: 10.1002/cjce.22104

Cozmuta, M. L., Cozmuta, A. M., Nicula, A. P. C., Nsimba, E. B., and Tutu, H. (2012). "The influence of pH on the adsorption of lead by Na-clinoptilolite: Kinetic and equilibrium studies," *Water SA* 38 (2), 269-278. DOI: 10.4314/wsa.v38i2.13

Crini, G. (2006). "Non-conventional low-cost adsorbents for dye removal: A review," *Bioresource Technology* 97(9), 1061-1085. DOI: 10.1016/j.biortech.2005.05.001

Demirbas, A. (2008). "Heavy metal adsorption onto agro-based waste materials: A review," *Journal of Hazardous Materials* 157(2-3), 220-229. DOI: 10.1016/j.jhazmat.2008.01.024

Deng, L., Su, Y., Su H., Wang, X., and Zhu, X. (2006). "Biosorption of copper (II) and lead (II) from aqueous solutions by nonliving green algae *Cladophora fascicularis*: Equilibrium, kinetics, and environmental effects," *Adsorption* 2(4), 267-277. DOI: 10.1007/s10450-006-0503-y

Erdem, M., Ucar, Karagöz, S., and Tay, T. (2013). "Removal of lead (II) ions from aqueous solutions onto activated carbon derived from waste biomass," *The Scientific World Journal* Article ID 146092, 1 – 7.

Ghasemi, M., Javadian, H., Ghasemi, N., Agarwal, S., and Gupta, V. K. (2016a). "Microporous nanocrystalline NaA zeolite prepared by microwave assisted hydrothermal method and determination of kinetic, isotherm and thermodynamic parameters of the batch sorption of Ni (II)," *Journal of Molecular Liquids* 215, 161-169.

Ghasemi, M., Mashhadi, S., Asif, M., Tyagi, I., Agarwal, S., and Gupta, V. K. (2016b). "Microwave-assisted synthesis of tetraethylenepentamine functionalized activated carbon with high adsorption capacity for Malachite green dye," *Journal of Molecular Liquids* 213, 317-325.

Hikmat, N. A., Qassim, B. B. and Khethi, M. T. (2014). "Thermodynamic and kinetic studies of lead adsorption from aqueous solution onto petiole and fiber of palm tree," *American Journal of Chemistry* 4(4), 116-124.

Imamoglu, M., and Tekir, O. (2008). "Removal of copper(II) and lead(II) ions from aqueous solutions by adsorption on activated carbon from a new precursor hazelnut husks," *Desalination* 228(1–3),108-113.

Iqbal, M., Saeed, A., and Zafar, S. I. (2009). "FTIR Spectrophotometry, kinetics, and adsorption isotherms modeling, ion exchange, and EDX analysis for understanding the mechanism of

Cd^{2+} and Pb^{2+} removal by mango peel waste," *Journal Hazardous Materials* 164(1), 161-171. DOI: 10.1016/j.jhazmat.2008.07.141

Issabayeva, G., Aroua, M. K., and Sulaiman, N. M. N. (2006). "Removal of lead from aqueous solutions on palm shell activated carbon," *Bioresource Technology* 97(18), 2350-2355.

Johns, M. M., Marshall, W. E. and Toles, C. A. (1998). "Agricultural byproducts as granular activated carbons for adsorbing dissolved metals and organics," *Journal of Chemical Technology and Biotechnology* 71(2), 131-140.

Khan, T. A., Ali, I., Vati Singh, V., and Sharma, S. (2009). "Utilization of fly ash as low-cost adsorbent for the removal of Methylene Blue, Malachite Green, and Rhodamine B dyes from textile wastewater," *Journal of Environmental Protection Science* 3, 11-22

Kikuchi, Y., Qian, Q., Machida, M., and Tatsumoto, H. M. (2006). "Effect of ZnO loading to activated carbon on Pb(II) adsorption from aqueous solution," *Carbon* 44(2), 195-202.

Kobya, M., Demirbas, E., Senturk, E., and Ince, M. (2005). "Adsorption of heavy metal ions from aqueous solutions by activated carbon prepared from apricot stone," *Bioresource Technology* 96(13), 1518-1521.

Li, K. Q., Zheng, Z., Zhang, J. B., and Mei, C. B. (2010). "Adsorption of lead ions onto activated carbon prepared from bio-plant stems activation with H_3PO_4," *Chin. J. Environ. Eng*. 4(6), 1238-1242.

Li, X., Tang, Y., Xuan, Z., Liu, Y., and Luo, F. (2007). "Study on the preparation of orange peel cellulose adsorbents and biosorption of Cd^{2+} from aqueous solution," *Separation and Purification Technology* 55(1), 69-75. DOI: 10.1016/j.seppur.2006.10.025

Lin, T. Y., Viswanathan, S., Wood, C., Wilson, P. G., Wolf, N., and Fuller, M. T. (1996). "Coordinate developmental control of the meiotic cell cycle and spermatid differentiation in *Drosophila* males," *The Company of Biologists Limited* 122, 1331-1341.

Liu, Y. (2009). "Is the free energy change of adsorption correctly calculated?" *Journal of Chemical Engineering Data* 54, 1981-1985.

Luduena, L., Fasce, D., Alvarez, A. D., and Stefani, P. M. (2011). "Nanocellulose from rice husk following alkaline treatment to remove silica," *BioResources* 6(2), 1440-1453.

Lugo-Lugo, V., Hernández-López, S., Barrera-Díaz, C., Ureña-Núñez, F., and Bilyeu, B. (2009). "A comparative study of natural, formaldehyde-treated and copolymer-grafted orange peel for Pb(II) adsorption under batch and continuous mode," *Journal of Hazardous Materials* 163(2–3), 1255-1264.

Mashhadi, S., Javadian, H., Ghasemi, M., Saleh, T., and Gupta, V. K. (2016a). "Microwave-induced H_2SO_4 activation of activated carbon derived from rice agricultural wastes for sorption of methylene blue from aqueous solution," *Desalination and Water Treatment* 57, 21091-21104.

Memon, S. Q., Memon, N., Shaw, S. W., Khuhawar, M. Y., and Bhanger, M. I. (2007). "Saw dust- A green economical sorbent for the removal of cadmium (II) ions," *Journal of Hazardous Materials* 39, 116-121.

Mouni, L., Merabet, D., Bouzaza, A. and Belkhiri, L. (2011). "Adsorption of Pb(II) from aqueous solutions using activated carbon developed from Apricot stone," *Desalination* 276(1–3), 148-153.

Naiya, T. K., Bhattacharya, A. K., and Das, S. K. (2009a). "Clarified sludge (basic oxygen furnace sludge) – An adsorbent for removal of Pb(II) from aqueous solutions – Kinetics, thermodynamics and desorption studies," *Journal of Hazardous Materials* 170, 252-262.

Naiya, T. K., Bhattacharya, A. K., and Das, S. K. (2009b). "Adsorption of Cd(II) and Pb(II) from aqueous solutions on activated alumina," *Journal of Colloidal and Interface Science* 333, 14-26.

Naiya, T. K., Chowdhury, P., Bhattacharya, A. K., and Das, S. K. (2009c). "Saw dust and neem bark as low-cost natural biosorbent for adsorptive removal of Zn(II) and Cd(II) ions from aqueous solutions," *Chemical Engineering Journal* 148(1), 68-79. DOI: 10.1016/j.cej.2008.08.002

Saeed, A., Akhter, M. W., and Iqbal, M. (2005). "Removal and recovery of heavy metals from aqueous solution using papaya wood as a new biosorbents," *Separation and Purification Technology* 45(1), 25-31. DOI: 10.1016/j.seppur.2005.02.004

Sarkanen, K. V., and Ludwig C. H. (1971). "Lignins: Occurrence, formation, structure, and reactions," *Journal of Polymer Science Part C: Polymer Letters* 10(3), 228-230. DOI: 10.1002/pol.1972.110100315

Sciban, M., Klasnja, M., and Skrbic, B. (2006). "Modified hardwood sawdust as adsorbent of heavy metal ions from water," *Wood Science and Technology* 40, 217-227.

Sciban, M., Radetic, B., Kevresan, Z., and Klasnja, M. (2007). "Adsorption of heavy metals from electroplating waste water by wood saw dust," *Bioresource Technology* 98(2), 402-409. DOI: 10.1016/j.biortech.2005.12.014

Sekar, M., Sakthi, V., and Rengaraj, S. (2004). "Kinetics and equilibrium adsorption study of lead (II) onto activated carbon prepared from coconut shell," *J. Colloid and Interface Science* 279(2), 307-313.

Seki, K., Saito, N., and Aoyama, M. (1997). "Removal of heavy metal ions from solutions by coniferous barks," *Wood Science and Technology* 31(6), 441-447. DOI: 10.1007/BF00702566

Sharifipour, F., Hojati, S., Landi, A., and Faz Cano, A. (2015). "Kinetics and thermodynamics of lead adsorption from aqueous solutions onto Iranian sepiolite and zeolite," *International Journal of Environmental Research* 9(3), 1001-1010.

Sharma, A., and Bhattacharyya, K. G. (2005). "*Azadirachta indica* (Neem) leaf powder as a biosorbent for removal of Cd(II) from aqueous medium," *Journal Hazardous Materials* 125(1-3), 102-112. DOI: 10.1016/j.jhazmat.2005.05.012

Singh, A. P. K., Srivastava, K. K., and Shekhar, H. (2009). "Arsenic (III) removal from aqueous solution by mixed adsorbent," *Indian Journal of Chemical Technology* 16, 136-141. DOI:

Singh, B., and Das, S. K. (2012). "Removal of Pb(II) ions from aqueous solution and industrial effluent using natural biosorbents," *Environmental Science and Pollution Research* 9(6), 2212-2226.

Singh, B., Bar, N., and Das, S. K. (2015). "The use of artificial neural network (ANN) for modeling of Pb(II) adsorption in batch process," *Journal of Molecular Liquids* 211, 228-232.

Tan, G., and Xiao, D. (2009). "Adsorption of cadmium ion from aqueous solution by ground wheat stems," *Journal Hazardous Materials* 164(2-3), 1359-1363. DOI: 10.1016/j.jhazmat.2008.09.082

Tran, H., and Chao, H. (2016). "Thermodynamic parameters of cadmium adsorption onto orange peel calculated from various methods," *Journal of Environmental Chemical Engineering* 4, 2671-2682.

Xu, T., and Liu, X. Q. (2008). "Peanut shell activated carbon: characterization, surface modification and adsorption of Pb^{2+} from aqueous solution," *Chinese Journal of Chemical Engineering* 16(3), 401-406.

Zeng, G., Liu, Y., Tang, L., Yang, G., Pang, Y., Zhang, Y., Zhou, Y., Li, Z., Li, M., Lai, M., He, X., and He, Y. (2015). "Enhancement of Cd(II) adsorption by polyacrylic acid modified magnetic mesoporous carbon," *Chemical Engineering Journal* 259, 153-160. DOI: 10.1016/j.cej.2014.07.115

Zhang, Y., Zhao, J., Jiang, Z., Shan, D. and Lu, Y. (2014). "Biosorption of Fe(II) and Mn(II) ions from aqueous solution by rice husk ash," *BioMed Research International* 2014, Article ID 973095, 1 – 10. DOI: 10.1155/2014/973095

Article submitted: August 14, 2016; Peer review completed: October 29, 2016; Revised version received and accepted: November 21, 2016; Published: December 5, 2016.
DOI: 10.15376/biores.12.1.799-818